*Cerebral Cortex*, May 2018;28: 1866–1881

**doi: 10.1093/cercor/bhy035**
Advance Access Publication Date: 22 February 2018
Original Article

ORIGINAL ARTICLE

# Directed Interaction Between Monkey Premotor and Posterior Parietal Cortex During Motor-Goal Retrieval from Working Memory

Pablo Martínez-Vázquez[1] and Alexander Gail[1,2,3]

[1]German Primate Center, Cognitive Neuroscience Lab, Kellnerweg 4, 37077 Göttingen, Germany, [2]Bernstein Center for Computational Neuroscience, Göttingen, Germany and [3]Faculty of Biology and Psychology, Georg-August-Universität, Göttingen, Germany

Address correspondence to Pablo Martínez-Vázquez, German Primate Center, Cognitive Neuroscience Lab, Kellnerweg 4, 37077 Göttingen, Germany. Email: pmvazquez@dpz.eu

## Abstract

Goal-directed behavior requires cognitive control of action, putatively by means of frontal-lobe impact on posterior brain areas. We investigated frontoparietal directed interaction (DI) in monkeys during memory-guided rule-based reaches, to test if DI supports motor-goal selection or working memory (WM) processes. We computed DI between the parietal reach region (PRR) and dorsal premotor cortex (PMd) with a Granger-causality measure of intracortical local field potentials (LFP). LFP mostly in the beta (12–32 Hz) and low-frequency ($f \leq 10$ Hz) ranges contributed to DI. During movement withholding, beta-band activity in PRR had a Granger-causal effect on PMd independent of WM content. Complementary, low-frequency PMd activity had a transient Granger-causing effect on PRR specifically during WM retrieval of spatial motor goals, while no DI was associated with preliminary motor-goal selection. Our results support the idea that premotor and posterior parietal cortices interact functionally to achieve cognitive control during goal-directed behavior, in particular, that frontal-to-parietal interaction occurs during retrieval of motor-goal information from spatial WM.

**Key words:** action selection, goal-directed behavior, Granger causality, motor planning, working memory

## Introduction

Cognitive control of action refers to capabilities which allow a subject to dissociate behavior from the kind of action that is immediately afforded by the sensory input. This includes flexible selection among alternative actions depending on the behavioral context as in decision making; but also action planning, a form of prospective working memory (WM) for withholding immediate action or planning of sequential actions. While sensory stimuli can evoke a strong urge to reach out for them (e.g., chocolate on the table), behavioral context determines which action is most adequate (grab the apple instead of the chocolate while mommy is still in the room). Cognitively controlled goal-directed selection of action requires integration of sensory and contextual cues. WM is required if we plan but withhold an immediate response to a sensory cue for later execution (wait until mommy left the room). Action selection and spatial WM have both been associated with the frontoparietal network (FPN) in the cerebral cortex of primates, particularly with directed interactions (DIs) between the frontal lobe and the parietal lobe, but their neural mechanisms remain unresolved. While some studies suggest a role of frontoparietal interactions in action selection (Pesaran et al. 2008; Praamstra

et al. 2009; Rawle et al. 2012; Nacher et al. 2013), others emphasize a role in WM (Tomita et al. 1999; Sauseng et al. 2005, 2010; Salazar et al. 2012; Dotson et al. 2014). Here we tested directly if directed signal interactions between arm-movement related dorsal premotor cortex (PMd; here: F2) in the frontal lobe (Matelli et al. 1991, 1998; Wise et al. 1997) and the parietal reach region (PRR; here: MIP) in the posterior parietal cortex (Colby et al. 1988; Shipp et al. 1998; Snyder et al. 2000; Lewis and Van Essen 2000a, 2000b) of rhesus monkeys are more consistent with a role in context-dependent action selection or in spatial WM operations during a reach task that required both.

The primate FPN is well suited to mediate between sensory-guided and context-regulated behavioral demands (Fuster 2001, 2009) since it can integrate input from prefrontal structures containing information about currently valid behavioral rules (Miller and Cohen 2001; Wallis and Miller 2003) with input from sensory association cortices providing information on the current sensory state (Mulliken et al. 2008). Sustained and spatially selective neural responses in areas PMd and PRR of the FPN during instructed delay tasks suggest that both areas contribute to arm-movement planning (Kalaska et al. 1997; Wise et al. 1997; Andersen and Cui 2009), at least in the sense that they can maintain effector-specific spatial motor-goal information in WM. And they do so in a context-specific manner. When a default response towards a visual target has to be substituted with an antireach away from the target, PRR and PMd encode spatial motor-goal information, not sensory target-related information, during motor planning (Crammond and Kalaska 1994; Gail and Andersen 2006; Gail et al. 2009). Equivalent observations can be made for antisaccades in the frontoparietal oculomotor areas (Schlag-Rey et al. 1997; Barash 2003; Munoz and Everling 2004; Zhang and Barash 2004). When the spatial constraints for a required movement are determined, that is, a set of potential reach goals has been identified, but the valid behavioral rule for selecting among these goals is yet undetermined, then PRR and PMd can encode multiple potential motor goals prior to choice (Cisek and Kalaska 2005; Klaes et al. 2011). This sustained co-encoding underlines the idea of a repertoire of potential motor goals which is associated with a given stimulus configuration (Klaes et al. 2012) and which is maintained active in the frontoparietal sensorimotor cortex until the task demands competitive selection among the potential goals by the subject (Cisek and Kalaska 2010; Cisek 2012).

The aforementioned examples emphasize the similarity of sustained spatio-temporal encoding between posterior parietal and premotor areas once subjects have settled on a single or multiple potential motor goals, but still have to withhold the corresponding response due to an instructed delay. In this sense, the widely distributed motor planning signals in the FPN are a form of WM maintenance (Funahashi et al. 1989; Chafee and Goldman-Rakic 2000). Such WM is prospective, that is, stores spatial information relevant for pending action, not preceding sensation (Lemus et al. 2007; Martinez-Garcia et al. 2011).

Due to anatomical connectivity, functional interaction between PRR and PMd should be expected. Numerous studies showed that projections to PMd (F2) originate from PRR (MIP) (Ghosh and Gattera 1995; Johnson et al. 1996; Petrides and Pandya 1999; Luppino et al. 2001, 2003; Marconi et al. 2001; Tanné-Gariépy et al. 2002; Markov et al. 2014), as well as from PPR (V6A) (Matelli et al. 1998; Caminiti et al. 1999; Gamberini et al. 2009). Injections in dorsal V6A (neighboring MIP and, according to some authors likely included in PRR) showed dense projections to rostral PMd (F7) and also F2; (Caminiti et al. 1999; Marconi et al. 2001; Gamberini et al. 2009; Bakola et al. 2010). While published studies with retrograde injections in MIP are lacking (Markov et al. 2014), preliminary data suggest projections from F2 to MIP not only disynaptically (Graf et al. 2006) but also monosynaptically (own observations, unpublished). Additionally, VA6 and MIP are mutually interconnected (Shipp et al. 1998; Gamberini et al. 2009; Passarelli et al. 2011), which together argues for bidirectional connectivity between PRR (MIP/V6A) and PMd.

But how do frontal and parietal areas functionally interact during preliminary selection of action, that is, when spatial and contextual cues are integrated for identifying one or multiple valid potential motor goals, or during final selection of action, that is, when choosing among multiple goals or confirming a preliminarily selected goal? The dynamic transition from sensory cue related to motor-goal related encoding in antireach tasks, as observed in PMd and PRR (Crammond and Kalaska 1994; Gail and Andersen 2006; Gail et al. 2009), marks a process of action selection by integrating spatial information (cue position) with contextual information (pro/anti rule). Latency analysis of neural spiking showed that PMd encodes context-dependent motor goals (antireach goals) earlier than PRR while behavioral response latencies (reaction times) correlated better with neural motor-goal latencies in PRR (Westendorff et al. 2010). This suggests that space-context integration (= preliminary motor-goal selection) might be achieved in frontal areas, but also that the resulting motor-goal information might be passed on to parietal cortex before action is executed. For this, frontal-to-parietal DI might be needed for final action selection prior to execution, not only, but particularly strongly in free-choice action selection (Pesaran et al. 2008).

On the other hand, defining a preliminary motor goal or updating it in the context of a delayed response task also implies a process of WM encoding; and final selection or confirmation of a motor goal after an instructed delay in a memory-guided task requires retrieval of motor-goal information from WM. Therefore, the functional role of interaction between premotor and posterior parietal cortex is not clear from the few reported cases. Here we compare DI between PRR (MIP) and PMd (F2) during rule-based motor-goal selection and memory-guided planning of goal-directed reaches to test its role in either aspect of cognitive control.

## Materials and Methods

### Behavioral Task

Two monkeys were trained in a memory-guided center-out antireach task (Westendorff et al. 2010). Each trial was composed of multiple phases (Fig. 1A). To start a new trial the monkey needed to maintain eye fixation (tolerance: 2.5–4° visual angle VA diameter; 224 Hz CCD camera, ET-49B, Thomas Recording, Germany) and hand fixation (2–6°VA) to the center of a touch-screen (IntelliTouch, ELO System, CA, USA) for 500–2000 ms (fixation period). Eye fixation had to be maintained for the rest of the trial, hand fixation until the "go" instruction. Eye and hand fixation targets were indicated by small (1.62° VA side length) horizontally adjacent square stimuli in red and white, respectively. In the example, condition of early spatial and early context instruction (ECES; Fig. 1A), a spatial cue about the reach target appeared during the pre-cue period (white filled circle of 3.2° VA, flashed for 200 ms). Spatial cues were randomly placed at one of 4 possible angular positions relative to the center of the screen (0, 90, 180, 270°) with a center eccentricity of 14.5° VA. Simultaneously, a green (pro) or a blue (anti) square frame appeared around the eye (red) and hand (white) fixation positions, specifying the spatial transformation rule valid in this trial (context cue). In proreaches

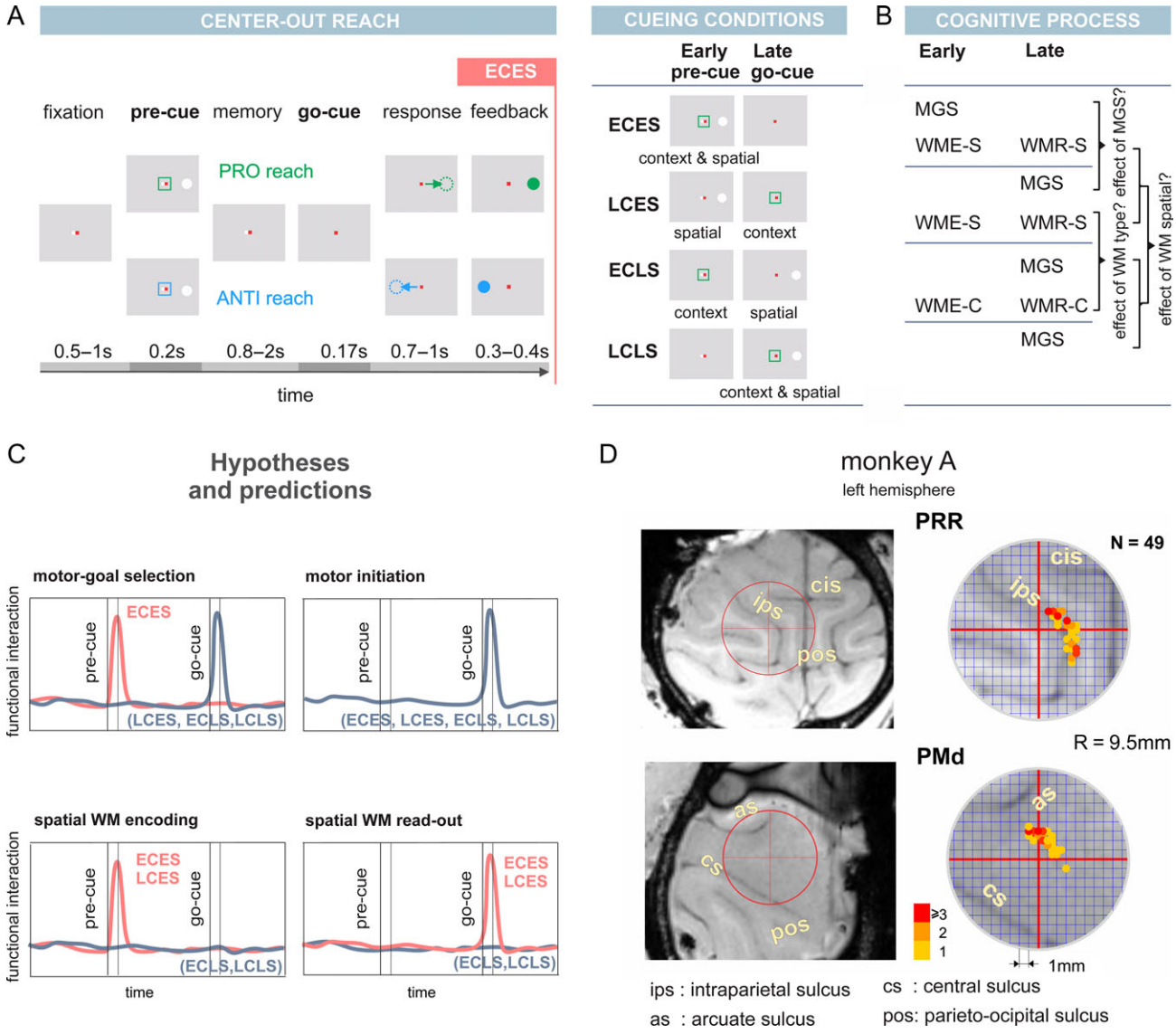


**Figure 1.** Task and recording sites (*A*) Time-line of the memory-guided center-out reach task in an example trial with early context (colored square, instructing pro- or antireach) and early spatial (white disc at 0, 90, 180, or 270° position) cueing (ECES condition). Set of all 4 possible cueing conditions, depending on the timing of the context and the spatial cue during the pre-cue and go-cue period, respectively. (*B*) Cognitive processes required at different times in the 4 cueing conditions (MGS – motor-goal selection, WME, working memory encoding (S: spatial, C: context), WMR, working memory retrieval) and relevant comparisons for identifying which process best explains any observed neural modulations between cueing conditions. (*C*) Hypotheses and corresponding predictions for the times at which frontoparietal interaction should occur according to its hypothesized role in motor-goal selection ( = space-context integration), motor initiation (motor-goal confirmation, efference copy), spatial WM encoding, or spatial WM retrieval. Note that our hypotheses do not make predictions about the direction of interaction (PMd→PRR or PRR→PMd), the relative amplitudes of functional interaction, the relevant LFP signal frequency band, or the precise temporal dynamics, but mostly about the timing within the trial. (*D*) Position of recording sites in parietal and premotor cortices in monkey A for all n recording sessions ($n = 48$) based on post-surgical MR imaging. Color coded legend indicates the number of electrode penetrations at each site. See Supplementary Figure S1 for an explanation of the tilted projections and corresponding data from monkey S. ips, intraparietal sulcus; cis, cingulate sulcus; pos, parieto-occipital sulcus; as, arcuate sulcus; cs, central sulcus.

the monkeys had to perform a reach to the spatial cue location after the later go-signal. In antireaches, the movement had to be executed to the opposite direction, that is, at 180° relative to the spatial cue location. This proanti dissociation allowed separating the visuospatial cue information from the spatial motor-goal information and required successful space-context integration for selecting the proper motor goal. After the pre-cue period, the visual and context cues disappeared for a random delay of 800–2000 ms (memory period). When the small white square for hand fixation disappeared (go cue), monkeys were requested to execute the reach within 700–1000 ms (movement period), and hold the goal location for at least 300–400 ms (target-hold period; tolerance: 3.0–7.4°VA) to obtain liquid reward and high-pitch auditory feedback. Brief visual feedback was provided at the location of the motor goal (re-appearance of visual cue stimulus). Failure in eye or hand fixation resulted in trial abortion, failure in timely reach goal acquisition in an unsuccessful trial, both with the consequence of not obtaining a reward and associated with a low-pitch auditory feedback.

In 4 different cueing conditions space-context integration occurred at different times during the trial. The spatial cue and the context cue could either be presented simultaneously during the pre-cue period (ECES: Early Context Early Spatial) as described in the example condition above (Fig. 1A, left panel),

or at other times (Fig. 1A, "cueing conditions" panel) as described in the following. The 4 cueing conditions were randomly presented in blocks of 10–20 trials.

- ECLS (Early Context Late Spatial): Context cue during the pre-cue period, spatial cue during the go-cue period; during the memory period only the context information is known and must be memorized; at the time of the go-cue, the spatial information can be integrated with the pre-existing context information.
- LCES (Late Context Early Spatial): spatial cue during pre-cue period, context cue during go-cue period; during the memory period only the spatial information is known; this cue information or the associated potential motor goals can be memorized (Klaes et al. 2011); at time of go-cue, context information can be integrated with pre-existing spatial information.
- LCLS (Late Context Late Spatial): both, context cue and spatial cue presented during the go-cue period. There is no memory period, only a correspondingly longer fixation period; space-context integration occurs at time of the go-cue.

Both animals were trained in parallel in this task by the same team of trainers, following the same protocol. Starting from naïve animals, the training protocol followed the phases: hand fixation, eye fixation, proreach movements, and antireach movements. Since we have no indications for relevant differences between animals regarding their training history or acquired cognitive strategy, we restrict our reported results to findings which were significant and consistent in both animals.

## Animal Preparation

Experimental procedures were described previously (Gail et al. 2009). Two adult male rhesus monkeys (*Macaca mulatta*) were trained to sit in a primate chair approximately 35–40 cm in front of a 19-inch LCD touch-screen monitor. During task execution eye movements were continuously measured with a video-based tracking system (ET-49B Thomas Recording, GmbH). The monkeys' head positions were stabilized using implanted titanium head holders. Two custom-fit recording chambers (3di, Jena, Germany) were implanted to each monkey's skull contralateral to the handedness of the monkeys. The implantation of each chamber, one for PRR and the other for PMd, was guided by pre-surgical MRI and confirmed by post-surgical MRI (Fig. 1D and Fig. S1). All surgical and imaging procedures were conducted under general anesthesia.

All experiments complied with institutional guidelines on Animal Care and Use of the German Primate Center, the European Directive 2010/63/EU, and German national law and regulations, and were approved by regional authorities where necessary.

## Neural Recordings

We recorded simultaneously from PRR and PMd in both monkeys ($n$ = 48 and $n$ = 37 sessions for monkey A and S, respectively) with multiple electrodes in each area in each session (Fig. 1D and Fig. S1).The $x$–$y$ electrode locations within the chamber were newly positioned in each recording session using the $xyz$-manipulator that holds the microdrive with sub-millimeters resolution. Color coded legend in (Fig. 1D and Fig. S1) indicates the number of electrode penetrations at each site. The chamber coordinates relative to cortex were extracted from post-surgical MRI, allowing navigation and positioning of penetration sites relative to anatomical landmarks, for example, along the medial wall of IPS for PRR (most likely MIP) recordings at a depth of approximately 3–7 mm from cortical surface, and halfway between pre-central dimple, arcuate spur and superior arcuate sulcus for PMd (most likely F2) recordings at approximately 0.5–2 mm below cortical surface.

Extracellular activity was recorded with 2–5 glass-coated tungsten-iridium microelectrodes lowered in each cortical area through epidural stainless steel guide tubes (Eckhorn minimatrix, Thomas Recording GmbH, Giessen, Germany), with horizontal inter-electrode separations of 300–1500 μm within each area. Neural data was acquired with a Plexon MAP system (Plexon Inc., Dallas, TX, USA).

Broad-band signals were pre-amplified (x20), band-pass filtered ([0.7–300 Hz], fourth order) and digitized at 1 kHz for extracting LFP. Occasional trials contaminated with signal saturation artifacts in LFP were removed, and occasional power line interference at 50 Hz was attenuated using a notch filter (fourth-order Butterworth), and posteriorly low-pass filter with a fourth order Butterworth of cutoff frequency at 90 Hz, as a standard filtering.

To assess that LFP activity was collected from areas PRR and PMd, single unit spike waveforms (SUA) were isolated and analyzed confirming the existence of sustained motor-related direction selectivity during movement planning in the ECES memory period (Supplementary Fig. S2 and Westendorff et al. 2010).

## Time-Frequency Power Spectral Density

The time-frequency power spectral density (PSD) of the LFP signal in each channel x, $S_{x,x}$ ($t$, $f$), was obtained by sliding an analysis window of 200 ms length and a shift of 40 ms between consecutive windows. The window length was chosen to be sufficiently short to detect and track the brief transient modulations of DI which we expected during cue-integration, motor-goal selection, or memory manipulation processes, while at the same time being long enough to provide enough data per window for a reliable estimation of the model parameters.

Spectral decomposition was achieved via time-domain autoregressive modeling, since this approach was most convenient for expanding towards Granger-causal analyses as we implemented them (see following section for equations). For each window, an autoregressive linear prediction model (AR) of fixed order ($P$ = 20) was estimated using the Yule-Walker algorithm. The AR fits the LFP signal based on its immediate history. The model order $p$ defines the number of free parameters and corresponds to the number of preceding signal samples used for estimating the current signal sample. The time-domain AR model is then transformed into the frequency domain with a Z-transformation (here equivalent to a discrete Fourier transformation, DFT) to decompose the different signal frequencies that constitute the signal. From the model, we obtained the PSD as a polynomial depending on the signal frequency $S_{x,x}(f)$. The polynomial PSD function was sampled with 1 Hz resolution over the frequency range [0–70 Hz].

## Time-Frequency Directed Transfer Function

We performed spectrally and temporally resolved Granger-causality analysis between pairs of LFPs, simultaneously recorded from PRR and PMd. LFP signals from separate electrodes within the same brain area were highly similar within sessions. To avoid artificially high-channel counts by spatial oversampling of a larger-scale signal source (multiple electrodes picking up overlapping signals), which would result in overestimation of statistical power, we only computed the model for a single inter-area channel pair per each session. We defined a representative composite channel pair by randomly selecting 2 channels in each trial within the same recording session.

For each composite signal pair, we fitted a multivariate autoregressive model (MVAR) of order $p$ with the same sliding-window approach as for PSD (eq. 1). The LFP pairs, at time (sample) $n$, $X(n) = [x_{PRR}(n) x_{PMd}(n)]^T$, were described by the linear MVAR (Akaike 1968) model with a temporally uncorrelated residual error $E(n) = [e_{PRR}(n) e_{PMd}(n)]^T$,

$$\sum_{k=0}^{P_{opt}} A_k X(n-k) = E(n) \quad (1)$$

where $A_k$ are the 2×2 coefficients matrices for delay k.

For each analysis window, we selected the optimal MVAR model order ($P_{opt}$) by estimating the model order that gives the minimum value of Akaike's final prediction error using the QR factorization method (Neumaier 2001; Luetkepohl 2005). The optimum model order was bounded in the range $p = [4, 20]$.

For spectral decomposition, the MVAR model was Z-transformed resulting in a set of 2×2 polynomial matrices depending on the signal frequencies, namely the transfer function matrix $\mathbf{H}(f)$:

$$X(f) = \left( \sum_{k=0}^{P} A_k e^{-j2\pi f k t} \right)^{-1} E(f) = \mathbf{H}(f) E(f). \quad (2)$$

Given the transfer function matrix $\mathbf{H}(f)$

$$\mathbf{H}(f) = \begin{bmatrix} H_{PRR\,PRR} & H_{PRR\,PMd} \\ H_{PRR\,PMd} & H_{PMd\,PMd} \end{bmatrix} (f) \quad (3)$$

and the covariance matrix $\Sigma$ of the residuals $E(n)$, defined as $\sum = \mathbb{E}\{E(n)E^T(n)\}$, where $\mathbb{E}$ is the mathematical expectation,

$$\sum = \mathbb{E}\{E(n)E^T(n)\} = \begin{bmatrix} \Sigma_{PRR\,PRR} & \Sigma_{PRR\,PMd} \\ \Sigma_{PRR\,PMd} & \Sigma_{PMd\,PMd} \end{bmatrix} \quad (4)$$

the 2×2 signals' spectral matrix $\mathbf{S}(f)$ is given by

$$\mathbf{S}(f) = \begin{bmatrix} S_{PRR,PRR} & S_{PRR,PMd} \\ S_{PRR,PMd} & S_{PMd,PMd} \end{bmatrix} (f) = X(f)X^*(f) = \mathbf{H}(f)\Sigma\mathbf{H}^*(f). \quad (5)$$

For each time window, the coherence spectrum $C(f)$ was computed as normalized cross-spectrum between PRR and PMd across trials:

$$C_{PRR-PMd}(f) = \frac{\mathbb{E}\left[ X^{trial}_{PRR}(f) X^{trial*}_{PMd}(f) \right]^2}{\left| S_{PRR,PRR}(f) S_{PMd,PMd}(f) \right|} \quad (6)$$

Hence, coherence is sensitive to power covariation and phase-consistency across trials between PRR and PMd signals for each frequency bin. As coherence is symmetric and does not provide directionality information about signal correlations, we used the directed transfer function (DTF) as estimator of the spectral Granger causality (Kaminski and Blinowska 1991; Kaminski et al. 2001). The functional directed ("Granger-causal") interaction from area $i$ to area $j$ is defined by

$$DTF_{i \to j}(f) = \frac{H^2_{ij}(f)}{[H^2_{ii}(f) + H^2_{jj}(f)]^{1/2}}. \quad (7)$$

This DTF function was sampled every 1 Hz over the frequency range [0–70 Hz]. Note, we also computed an alternative version of Granger causality given by Geweke (1982), but the reported results are robust against this variation, such that the conclusions of our study do not depend on the specific formulation of the Granger causality measure. Takahashi and colleagues indicated that both measures, the Gewecke's formulation and DTF, at each frequency can be associated with a mutual information rate (Takahashi et al. 2010; Chicharro 2011). Additional to this indication of robustness, we show data from both animals separately to emphasize their similarity in terms of the functional interaction patterns, and restrict our report to results significantly and consistently showing in both animals.

## Significance Testing of DTF and DI Index

The causality estimators derived from the parametric MVAR model, such as the DTF, have non-linear relationships to the time series and their model residuals. The distributions for the estimator are not well known. It is therefore difficult to infer their statistical significance with analytical methods and to correct the causality estimators to compensate for potential effects of slow signal covariations or biases in noise or signal power that could be present in the data. Hence, we estimated functional interaction from the DTF function by comparing it against a null distribution computed from phase-scrambled LFP surrogates, as illustrated in Supplementary Information S2.

Supplementary Figure S2A shows example trials of pairs of LFP from PRR and PMd for a specific time epoch within a trial of a single recording session. We computed surrogate LFPs (Supplementary Fig. S3B) with the same PSDs as the original LFP data, but with randomized phase (Kaminski and Blinowska 1991; Kaminski et al. 2001). The random-phase surrogate method (Osborne et al. 1986; Theiler et al. 1992) is a three-step procedure: 1) Take a discrete Fourier transform of the data. 2) Independently and uniformly randomize the phase values between $[-\pi, \pi]$ for each signal frequency. 3) Apply the discrete inverse Fourier transform to back-transform into the time domain. Any systematic temporal interdependence existing in the simultaneous recorded pairs of the original data is eliminated by the phase randomization in the surrogate data. Since LFP power changes over the time course of a trial, we compared DTF against the surrogate DTF separately for each time window. With this approach, we tracked the potential influences of LFP power changes, on the causality measure at each analysis time, such that the resulting DTF is independent of power. Each $DTF_{i \to j}(t, f)$ estimator was corrected by the surrogate estimation, obtaining the DI index $DI_{i \to j}(t, f)$, as follows. For a given pair of signals, and a given trial $l$ we generated $N_{SURR}$ surrogate pairs ($N_{SURR} = 20$) and their DTF functions were calculated, $surrDTF^l_{ns,i \to j}(t, f)$ with ns = 1…$N_{SURR}$ (Supplementary Fig. S2C). The mean of the surrogate ensemble surrDTF functions was calculated:

$$\overline{surrDTF}^l_{i \to j}(t, f) = \frac{1}{N_{SURR}} \sum_{ns=1}^{N_{SURR}} surrDTF^l_{ns,i \to j}(t, f). \quad (8)$$

The DI per each recording session, $DI^{session}(t, f)$ with $L$ trials, was defined as the difference of the DTF function from their mean surrogate DTF across all trials (Supplementary Fig. S3D and E):

$$DI^{session}_{i \to j} = \frac{1}{L} \sum_{l=1}^{L} DI^l_{i \to j}(t, f) - \overline{surrDTF}^l_{i \to j}(t, f). \quad (9)$$

We do not report significances of single DI values, for which we would test the DTF value against the surrogate distribution. Rather, the results presented bellow will refer to the distribution of the DI across all recording sessions (Fig. S3F). DI for each time window and signal frequency is reported as result if the mean of this DI distribution was significantly larger than zero, corresponding to a paired $t$-test of DFT against the mean surrDTF across sessions.

## Results

### Working Hypotheses and Neural Predictions

The task required integration of a spatial cue (S) with context (C) to determine the motor goal at different times during the 4 trial types (Fig. 1B). From previous analyses of neural spike data in this task, we know that neurons in PMd and PRR encode the instructed motor-goal location within 150–200 ms after an ECES pre-cue, or after any missing information is completed with the second cue in the 3 other cueing conditions (Westendorff et al. 2010). The fact that sustained neural activity during the memory period is selective for the pending reach movement rather than the preceding sensory instruction supports the view that the maintained WM content in the FPN marks prospective information in our task, i.e., that the WM content consists of the spatial motor goal. Therefore, we consider "prospective WM" the more abstract cognitive state or process, while in the given task the "spatial motor goal" could be seen as the content of the WM. In this sense, WM retrieval could serve the function of re-activating the motor goal representation.

Example data from single neurons of each animal and brain area of the current data set demonstrate that spatial motor-goal selectivity is present during the memory period in ECES but not LCLS trials, confirming that preliminary motor-goal selection occurs during the pre-cue in ECES trials (Supplementary Fig. S2).

Depending on its functional role, DI between PRR and PMd could occur during the sustained memory phase (motor planning/WM maintenance) or transiently in response to the early or late instruction cues. Different transient interaction patterns across the 4 cueing conditions should be expected for our different working hypotheses (Fig. 1B and C): 1) the motor-goal selection hypothesis predicts DI during the pre-cue in ECES trials and during the go-cue in all other cueing conditions (Fig 1C). A comparison between the ECES and the LCES condition will be most informative about motor-goal selection signals, since the 2 conditions require motor-goal selection at different times while matching in terms of spatial WM processing (Fig. 1C). 2) The spatial WM encoding hypothesis predicts interaction during the pre-cue only when spatial information is provided (ECES and LCES), with no interaction during the go-cue in any condition. 3) Correspondingly, the spatial WM retrieval hypothesis predicts interaction during the go-cue when spatial information is provided with the pre-cue (ECES and LCES) and needs to be retrieved for action execution at the time of the go-cue. Comparisons of the ECES and LCES conditions with the 2 other conditions during the pre-cue or go-cue will be most informative about spatial WM encoding and WM retrieval signals, respectively. 4) In analogy to spatial WM, context processing could engage WM activity in the ECLS condition. A comparison of the LCES and ECLS conditions will reveal differences in neural processing due to different memory content. Since non-spatial information is known to modulate neural responses in PMd and PRR hardly on its own, but mostly only in combination with spatial encoding (Stoet and Snyder 2004; Gail et al. 2009; Coallier et al. 2015), we do not predict specific signatures of WM processing related to memorizing of context information in our data. 5) Finally, transient interaction after the go-cue event, independent of the cueing condition, could occur but would be less conclusive. This is because manifold processes related to final goal selection, motor initiation, release from response inhibition, and forward model predictions can occur at this time.

### Behavioral Performance

Both animals showed high performance on the task. Behavioral results were reported before, when the neural tuning and latency results of the accompanying neural spiking activity were presented (Westendorff et al. 2010), and are repeated here for completeness. The average performance of monkey A was 86/86% (pro/anti) in the ECES condition, 85/84% in the LCES condition, 85/83% in the ECLS condition, and 86/85% in the LCLS condition, for monkey S it was 77/77% (pro/anti) in the ECES condition, 79/79% in the LCES condition, 75/75% in the ECLS condition, and 80/79% in the LCLS condition. Errors were mainly caused by ocular fixation breaks, not by incorrect target choices. The choice of reach target was correct in 97% for monkey S, and in 99% for monkey A.

### Low and Beta-Range Frequencies Dominate LFP Signals and Interaction

The main result of our study and prominent basic features of LFP can be seen already from a single example pair of electrodes in PRR and PMd during the ECES condition (Fig. 2). Two spectral components dominated the LFP signals: the beta-band (13–28 Hz, LFP-beta) and frequencies lower than 10 Hz (LFP-LF). Consistent with our previous observations (Chakrabarti et al. 2014), LFP-beta was stronger in PRR than PMd, as obvious already from simultaneously recorded raw data (Fig. 2A; see Supplementary Fig. S4A for raw data from other monkey) and corresponding power spectral densities (Fig. 2B). Otherwise, PRR and PMd showed similar spectro-temporal LFP features.

When local processing within both brain areas gives rise to LFP signals with sufficient power in a specific frequency band, then this allows quantifying mutual signal dependencies as a proxy for functional interaction (see Supplementary Fig. S5 for a discussion of spectral power). As LFP power itself, LFP coherence indicated that LFP-LF and LFP-beta are the major frequency bands potentially relevant for functional connectivity in our data. Since coherence is normalized to power separately at each signal frequency it could indicate signal coupling also for frequencies with less power. Depending on how coherence was computed, at frequencies higher than LFP-beta coherence did not or did barely exceed the random level of the surrogate data (Supplementary Fig. S6). This is why we will mostly focus on results from frequencies of the beta range or lower in the following, which were more robust than results from gamma frequencies.

### Directed Functional Interaction Between PRR and PMd

The main features of DI can already be seen from the example pair of electrodes of one recording session in the ECES condition (Fig. 2C). The 2 transfer functions DI(PRR→PMd) and DI (PMd→PRR) have commonalities with coherence in terms of prevalent frequencies and temporal structure, but provide further insight due to their directionality. DI-beta occurred in PRR-to-PMd interaction in a sustained fashion during fixation and memory. DI-LF occurred in PMd-to-PRR interaction transiently in response to the go-cue (see Supplementary Fig. S4B for an example from monkey S). DI at frequencies higher than 35 Hz were sporadic.

The average DI across all recording sessions (Fig. 3A and B) is largely consistent between both monkeys and confirms the interaction pattern of the examples. During steady phases, like the memory period, DI-beta (PRR→PMd) was most prevalent, but also DI-gamma (PRR→PMd) appears slightly greater than zero around 40 to 45 Hz. In response to transient cue events, DI-beta (PRR→PMd) and DI-gamma (PRR→PMd) reduced with a downward sweep in peak frequency during recovery. DI – LF(PMd→PRR), on the other hand, only occurred in response to the go-cue, during

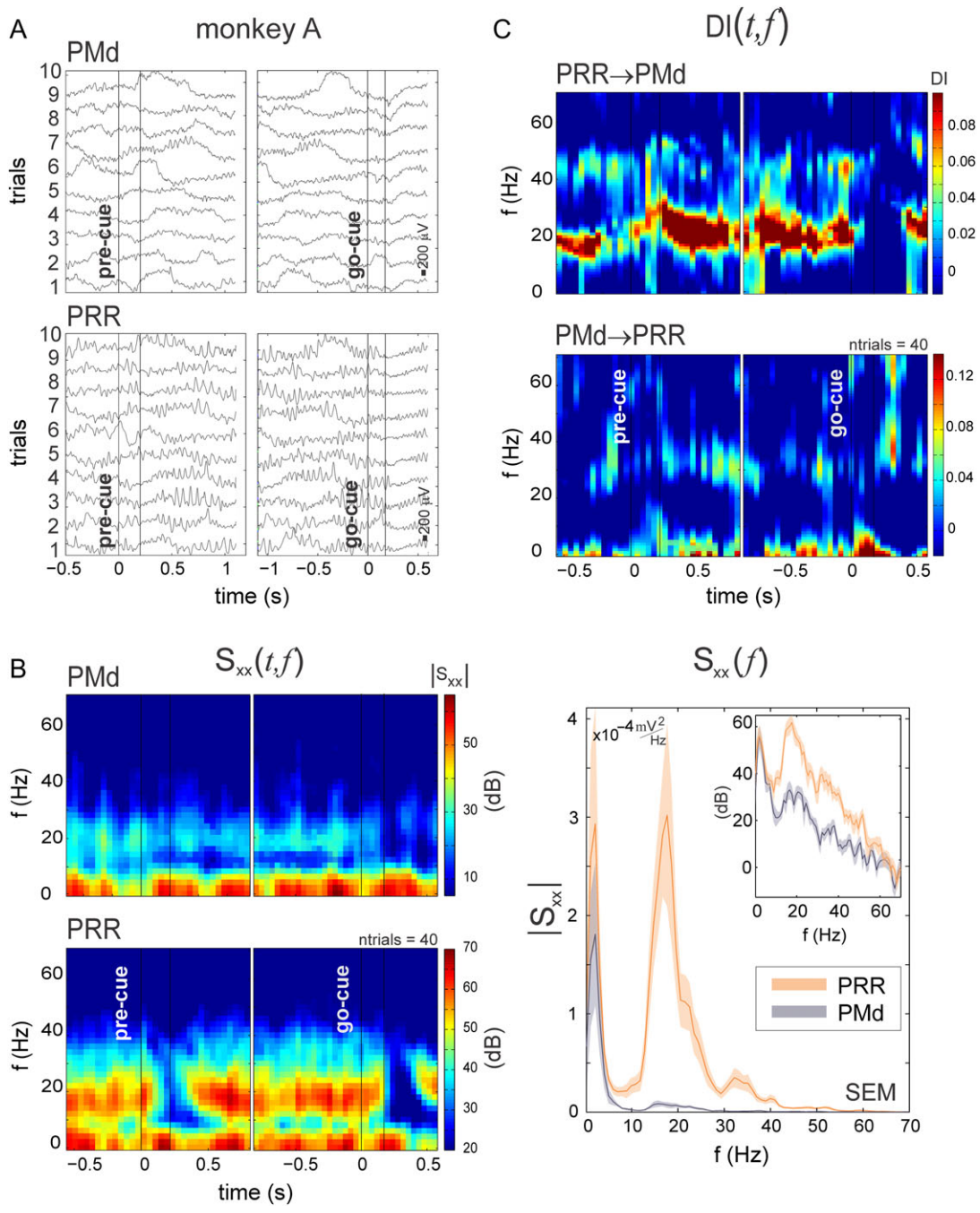


**Figure 2.** Raw data, spectral power, and example DI (*A*) Example of 10 simultaneous raw LFP traces acquired from PRR and PMd during proreaches to the 180° direction with ECES cueing (monkey A). Data were aligned to the pre- and the go-cue events (left panel and right panel, respectively). (*B*) Time-frequency spectrogram, $S_{xx}(t, f)$ of the raw LFP in PRR and PMd aligned to pre-cue and go-cue; average of 40 trials of the same recording session as in (A). Right panel, average LFP PSD during the late memory period, [−0.5, 0 s] aligned to go-cue (curve and shading show mean ± SEM). (*C*) Time-frequency DI between PRR and PMd for one single recording session. Upper panel contains the functional interaction from parietal to premotor while the lower panel shows the reverse interaction.

which DI-beta and DI-gamma were particularly low, and not during the pre-cue.

## Low-Frequency Functional Interaction from PMd to PRR During Spatial WM Retrieval

Of particular interest for our research goal was the question how DI depended on the cognitive processes happening at different times during the trial in the different cueing conditions. While the 4 cueing conditions overall showed similar spectro-temporal DI patterns (Supplementary Fig. S7A), there were also highly selective differences.

DI – LF(PMd→PRR) showed a prominent transient peak in response to the go cue in both monkeys with variable amplitude depending on cueing condition (Fig. 3C and *D*). There was no modulation of DI-LF after the pre-cue in any of the 4 cueing conditions, neither in the proreaches (Fig. 3C and *D*), nor in antireaches (data not shown). This temporal pattern of DI-LF

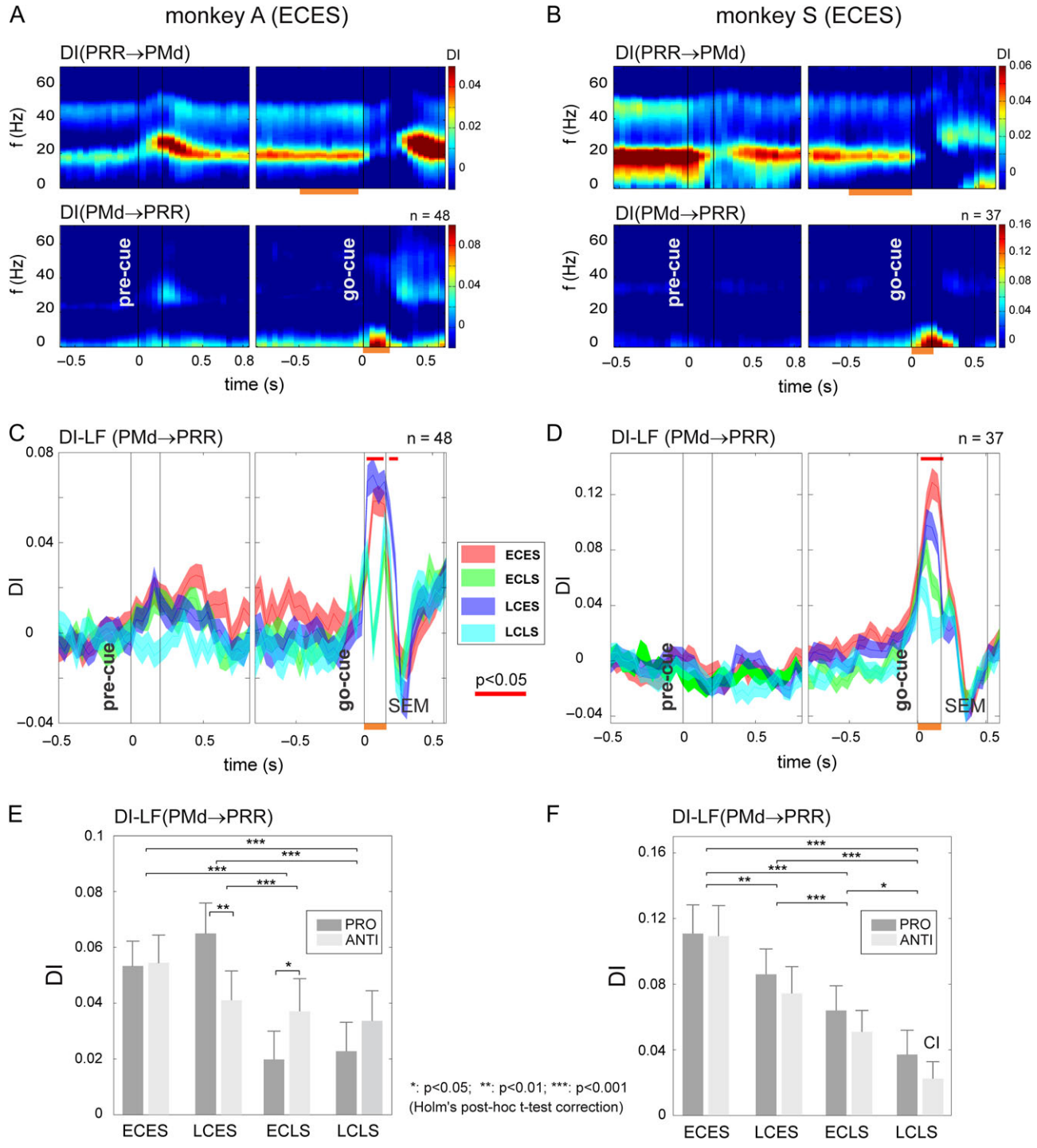


**Figure 3.** Frontoparietal DI of LFP signals. (*A*,*B*) Average time-frequency DI for proreaches in the ECES cueing condition across $n = 48$ and $n = 37$ sessions, monkey A and S, respectively. Orange bars below time-axis outline the DI test periods, ([−0.5, 0 s] before go-cue) for the memory epoch and ([0, 0.2 s] after the go-cue) for the go-signal. (*C*,*D*) Time evolution of the DI-LF(PMd→PRR) in proreaches of all cueing conditions (mean ± SEM). Upper red bar indicates significant difference between cueing conditions (one-way ANOVA with factor CUEING, $P < 0.05$). (*E*,*F*) Comparison of DI − LF(PMd→PRR) strength, for all cueing conditions and both contexts after go-cue onset [0–0.2 s] (mean ± 95% CI).

contradicts both, the motor-goal selection hypothesis and the WM encoding hypothesis, since for both hypotheses DI would have to be expected in response to the pre-cue at least in one (ECES; motor-goal selection hypothesis) or in 2 conditions (ECES, LCES; WM encoding hypothesis), respectively.

To test the WM retrieval hypothesis against the motor initiation hypothesis, we compared the DI − LF(PMd→PRR) in response to the go cue (period of 0.2 s following go-cue onset) between all conditions (Fig. 3*E* and *F*). DI − LF(PMd→PRR) did not depend on the factor CONTEXT, but varied with the factor

CUEING in both animals (2-way ANOVA with factors CUEING and CONTEXT; monkey A: Fcue(3,376) = 14.08, $P < 0.001$; Fcon (1,376) = 0.46, $P$ = n.s; Fcue × con (3,376) = 6.34, $P < 0.001$; monkey S: Fcue(3,288) = 37.8, $P < 0.001$; Fcon (1,288) = 3.4, $P$ = n.s.; Fcue × con(3,288) = 0.28, $P$ = n.s.). Importantly, in both monkeys each of the 2 spatial WM conditions (ECES, LCES) showed higher DI – LF(PMd→PRR) compared with the 2 conditions (ECLS, LCLS) when no spatial WM was required. Trials which required context WM (ECLS) compared with trials which required spatial WM (LCES, ECES) showed lower DI – LF(PMd→PRR), suggesting that mainly spatial WM retrieval triggers frontoparietal interaction, not WM processes per se. This means, the pattern of DI – LF(PMd→PRR) is most consistent with the spatial WM retrieval hypothesis.

Note, even though significantly weaker, both conditions without spatial WM retrieval (ECLS, LCLS) also lead to transient changes in DI – LF(PMd→PRR) in response to the go cue. This could indicate a baseline level of frontoparietal DI common to all conditions at the time of motor initiation, on top of which DI specific for WM retrieval occurs.

## Beta- and Gamma-frequency Functional Interaction from PRR to PMd During Holding States

DI(PRR→PMd) was most prominently seen in the beta-frequency band. For statistical comparisons, we calculated DI-beta, where "beta" was defined as the frequency of maximum DI (narrow band of 18–22 Hz in both animals) within the beta range. During the memory period ([−0.5, 0 s] aligned to the go-cue) DI – beta(PRR→PMd) was significant in all cueing conditions and both contexts, while DI-beta(PMd→PRR) was absent in both monkeys (Fig. 4A and B). Neither cueing condition nor context had a main effect on DI-beta (PRR→PMd) in either animal: monkey A (2-way ANOVA with factors CUEING and CONTEXT, Fcue(3,376) = 0.18, $P$ = n.s.; Fcon(1,376) = 0.16, $P$ = n.s.; Fcue × con(3,376) = 0.73, $P$ = n.s.) and monkey S (Fcue(3,288) = 0.52, $P < 0.01$; Fcon(1,288) = 0.25, $P$ = n.s.; Fcuexcon(3,288) = 1.19, $P$ = n.s.). Also, DI-beta (PRR→PMd) pooled across both animals was not significant (2-way ANOVA with factors CUEING and CONTEXT, Fcue(3,575) = 0.97, $P$ = n.s.; Fcon(1,575) = 2.3, $P$ = n.s.; Fcue × con(3,575) = 0.01, $P$ = n.s.).

Remarkably, in the LCLS condition prior to the go-cue, that is, when no information about the current trial was yet presented to the monkeys, DI-beta (PRR→PMd) was at least as strong (or slightly higher, monkey S) as in the other conditions, in which spatial WM had to be maintained (Fig. 4). This indicates that DI-beta is not specific for spatial or context-related information processing, but is more generally observed during states in which the animal withholds movement.

DI (PRR→PMd) was partly also seen in the gamma frequency band in both monkeys, but with much lower strength than DI-beta (see Supplemental Fig. S7). As DI-beta (PRR→PMd), the DI-gamma (PRR→PMd) did not vary significantly across cueing conditions and context conditions consistently in both animals: monkey A (2-way ANOVA with factors CUEING and CONTEXT, Fcue(3,376) = 0.40, $P$ = n.s.; Fcon(1,376) = 0.17, $P$ = n.s.; Fcuexcon (3,376) = 0.92, $P$ = n.s.) and monkey S (Fcue(3,288) = 0.34, $P$ = n.s.; Fcon(1,288) = 0.32, $P$ = n.s.; Fcuexcon(3,288) = 0.33, $P$ = n.s.). Similarly, DI-gamma (PMd→PRR) did neither reach significance for either of the 2 factors, nor their interaction.

In summary, DI results revealed 1) no relevant DI in response to the pre-cue, not even with the fully informative ECES pre-cue, 2) a sustained but task-parameter independent DI from PRR to PMd in the beta-frequency range during holding states, and 3) transient DI from PMd to PRR in the low-frequency band in response to the go-cue in all cueing conditions, but most strongly in conditions which required spatial WM retrieval.

## Behavioral Correlates of Frontoparietal DI

So far, we implied differences in the animals' cognitive processing between the cueing conditions based on the fact that the task design demanded different cognitive processes and animals performed correctly. Since the 4 different cueing conditions vary in terms of the cognitive demands prior to response initiation, the varying demand should also affect the animals' overt behavior. Via such behavioral indicator, we could then link the observed pattern of frontoparietal interaction more directly to differences in internal cognitive state. In the following we show that variations in DI were in fact linked to differences in reaction time (RT) between cueing conditions, while RT differences themselves did not explain DI differences, supporting the notion that frontoparietal DI reflects processes of cognitive control.

RT differences in our data indicate different cognitive demand prior to response execution when monkeys integrated go-cue with pre-cue information (Fig. 5A and B). The RTs are modulated by both, cueing condition and context, where modulation by cueing condition differed between the 2 contexts and also between the 2 animals (2-way ANOVA, interaction factor between CUEING × CONTEXT: Fcue × con(3,376) = 13.85, $P < 0.001$ for Monkey A,

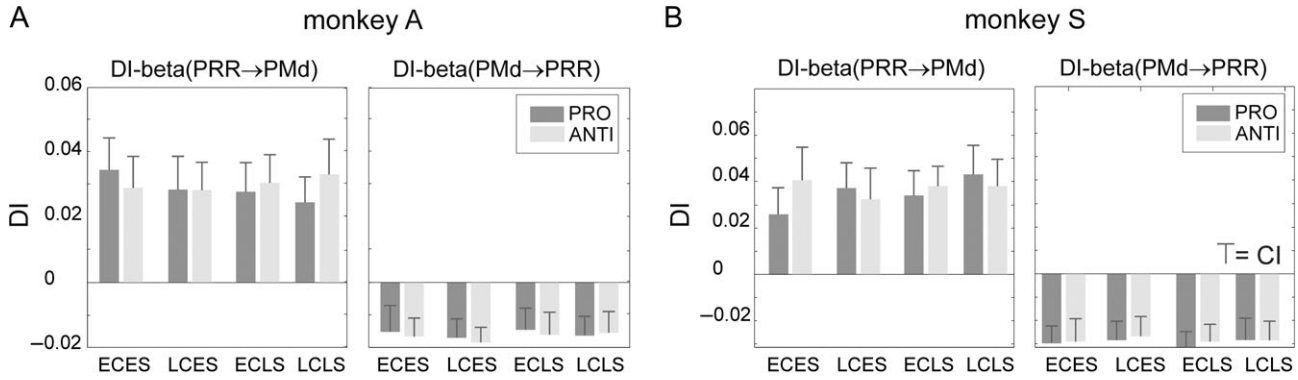


**Figure 4.** Functional DI at beta frequencies. (*A*,*B*) DI-beta for all 4 cueing conditions and both contexts (conventions as in Fig. 3E and F) during the late memory period [−0.5, 0 s] before the go-cue (mean ± 95%CI). DI-beta was evaluated at the narrow band within the beta range where DI had its maximum activity, which was 18–22 Hz in both animals).

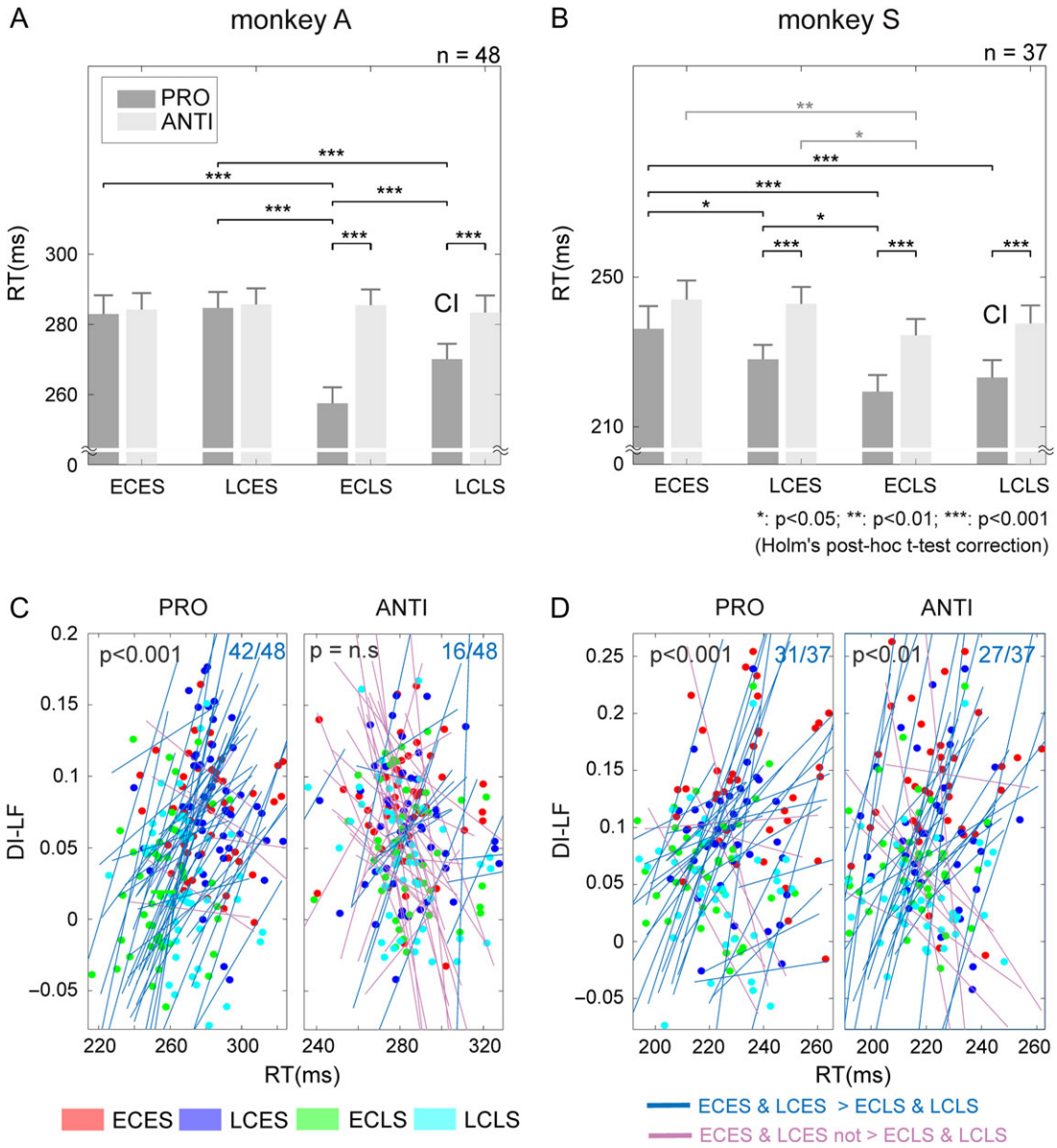


**Figure 5.** Strength of DI – LF(PMd → PRR) correlated with monkeys' RTs. (*A*,*B*) Average RTs in the 4 different cueing conditions and both contexts (conventions as in Fig. 3*E* and *F*). (C, D) DI-LF [0–0.2 s] after go-cue onset compared with RT for all recording sessions and colored for the cueing condition. Each point represents the mean LF-DI and mean RT within a session; the lines represent the linear regressions between mean LF-DI and mean RT per each session (4-point regression across cueing conditions). The blue lines correspond to those recordings that led to positive regressions, indicating that DI-LF and RT for the 2 spatial WM conditions (ECES, LCES) were higher than for the other 2 cueing conditions. 42/48 and 31/37 of the proreach trials for monkey A and S, respectively, showed such positive regression. Antireach trials in monkey S show similar proportion 27/37, while antireach trials in monkey A led less often to a positive regression. The *P*-values indicate the significance of the linear mixed-random effect model between the DI and the RT with the recording session as a random effect.

and Fcue × con(3,288) = 1.2, *P* = n.s. for monkey S). RTs in proreaches showed substantial differences across cueing conditions in each monkey (ANOVA with factor CUEING: $F(3,189) = 27.2$, $P < 0.001$ and $F(3,149) = 8.6$, $P < 0.001$ for monkey A and S, respectively). RTs in antireaches instead were independent of cueing condition in monkey A ($F(3,188) = 0.14$, *P* = n.s.) but modulated by cueing condition in monkey S ($F(3,149) = 3.5$, $P < 0.05$). In the 3 cases in which RT depended on cueing condition (monkey A: pro context, monkey S: pro and anticontext), RT was higher (post hoc *t*-test with Holm's correction) in the 2 conditions which required spatial WM (ECES, LCES) compared with conditions (ECLS, LCLS) which did not require spatial WM (Fig. 5*A* and *B*). In other words, while spatial WM and context had an impact on RT, the impact of spatial WM on RT was particularly obvious when reactions were not overall slowed down by the requirement to perform an antireach (the latter being the case in monkey A).

The first conclusion that can be derived from this observation is that differences in DI – LF(PMd→PRR) cannot be in general explained by RT differences, since the RT differences between the pro and anticontext seen in several cueing conditions across the 2 monkeys were not reflected in corresponding DI – LF(PMd→PRR) differences (Fig. 3*E* and *F*). This argument will be further strengthened quantitatively below. Second, within each animal and context, differences in RT between different cueing conditions could indicate differences in cognitive demand due to WM processing or differences in cue-integration

demands. Both differences in cognitive demand, due to cue integration or due to WM processing, could potentially require different frontoparietal interaction. Yet, sensory processing and cue-integration demands were shown above to not influence DI – LF(PMd→PRR) since there were no differences in DI between cueing conditions at the time of the pre-cue.

If DI – LF(PMd→PRR) reflects spatial WM retrieval, then we should expect higher DI with higher spatial WM demand, at least as long as higher RTs indicate such higher WM demand between different cueing conditions. This predicts that only modulation of RTs across cueing conditions (as indicator of varying WM demand) should correlate with DI. In contrast, RT variations due to random session-by-session variability should not correlate with DI.

Our results from a regression analysis and a linear mixed-effect model match these predictions. Figure 5C and *D* shows the linear regressions between DI – LF(PMd→PRR) and RT (both averaged across all trials of each cueing condition separately per each recording session, resulting in a 4-point regression across cueing conditions for each context). The blue lines correspond to positive regressions, indicating that DI-LF and RT for spatial WM conditions (ECES, LCES) were higher than for the other 2 conditions. 42/48 and 31/37 of the proreach sessions for monkey A and S, respectively, showed a positive regression. Antireach trials in monkey S show similar regression results, while antireach trials in monkey A less often led to a positive regression.

To confirm that DI – LF(PMd→PRR) is modulated by task-induced cognitive demand across conditions, and not by random fluctuations of RT across sessions, we computed a linear mixed-effect model (LME) with the session factor as a random effect, RT~D1 + (1|SESSION) + (DI−1|SESSION). The LME model confirmed a positive linear relationship between RT and DI-LF in proreaches for the monkey A ($\beta = 156.71$, $t(190) = 7.9$, $P < 0.001$) and monkey S ($\beta = 83.07$, $t(146) = 5.48.5$, $P < 0.001$), and in antireaches for monkey S ($\beta = 38.62$, $t(146) = 3.65$, $P < 0.01$) , but not for antireaches of monkey A ($\beta = -15.44$, $t(190) = -1.01$, $P$ = n.s.). As a control, none of the LME models with the cueing condition instead of session number as random factor (RT~DI + (1|CUE) + (DI − 1|CUE)) showed statistical significance: monkey A (proreach $\beta = -13.10$, $t(190) = -0.47$, $P$ = n.s., antireach $\beta = -25.54$, $t(190) = -1086$, $P$ = n.s.) and S (proreach $\beta = -25.73$, $t(146) = -1.09$, $P$ = n.s., antireach $\beta = -0.37$, $t(146) = -0.017$, $P$ = n.s.). This confirms that DI differences are not explained by RT differences within conditions across sessions.

In summary, the link between DI and RT shows that the observed frontal-to-parietal DI-LF (PMd→PRR) is not simply a by-product of RT differences per se. Instead DI-LF (PMd→PRR) occurs prior to movement onset most prominently in combination with retrieval of spatial WM, and is modulated in strength with the cognitive demand associated with this retrieval as inferred from differences in RT across cueing conditions.

## Discussion

Our goal-directed reach task required monkeys to select reach goals according to learned spatial transformation rules, and to maintain different information in WM during an instructed delay. We found directed functional interaction in the FPN in 2 distinct frequency bands of intracortical local field potentials (LFP): 1) A parietal-to-frontal interaction from PRR to PMd in the beta-frequency range (and similarly in the gamma frequency range, but weaker), present in a sustained fashion during trial periods which required the monkeys to hold a current state (fixation or memory), and with no dependency on cueing condition and 2) a frontal-to-parietal interaction at frequencies lower than 10 Hz, transiently present in response to the go cue, and modulated in strength by the task condition. Our findings suggest a role of frontal-to-parietal DIs in retrieval of motor-goal information from spatial WM.

### Frontal-to-Parietal Interaction in Low-frequency LFPs Is Not Consistent with a Role in Motor-Goal Selection

Our task required the monkeys to integrate visual spatial and color information to successfully select a reach goal. We expected a large-scale cortical integration process for proper choice of action, since the 2 types of information were qualitatively different. Spatial target stimuli have immediate meaning in reach tasks in the sense that animals are used to reach towards visual targets in daily live, and hence such stimulus has a high affordance for reaching to it. Accordingly, fastest reaches were achieved when the object appeared suddenly and the monkeys were allowed to directly reach towards a visible target without instructed delay (here: proreaches with late spatial cue; Fig. 5). The color cue, on the other hand, became meaningful to the animals only in the context of the proanti task through training. Color defined a trial-by-trial behavioral context which set the rules for translating the spatial cue position into a reach goal. While encoding of spatial visual target information is fast and omnipresent along the visuo-dorsal stream (Johnson et al. 1996; Pesaran et al. 2008; Westendorff et al. 2010; Battaglia-Mayer et al. 2014), selectivity for learned symbolic cues is typically associated with frontal lobe association cortex (Petrides 1982; Rowe and Passingham 2001; Toni et al. 2001; Wallis et al. 2001; Wallis and Miller 2003; Moisa et al. 2012), and only weakly present in explicit form during the memory period in PRR (Gail and Andersen 2006; Gail et al. 2009). Also, spatial motor-goal encoding emerges up to 40 ms later in PRR than PMd during antireaches (Westendorff et al. 2010), which means, if at all, then parietal motor-goal encoding should be contingent upon frontal lobe input, but not vice versa. Also, other studies showed transient frontal-to-parietal interaction at low signal frequencies during reach target selection in monkey (Pesaran et al. 2008; Nacher et al. 2013) (Pesaran, Nelson et al. 2008) and human (Praamstra et al. 2009; Rawle et al. 2012), suggesting a role in action selection and decision making. Hence, we expected frontal-to-parietal functional interaction to occur during space-context integration for motor-goal selection in our task.

Yet, based on our current results, we have to reject the cue integration or motor-goal selection hypothesis. In conditions in which both cues were presented prior to an instructed delay (ECES), no functional DI was found in response to the pre-cue, in neither anatomical direction and neither frequency band of LFP. But we know that monkeys must have achieved cue integration and motor-goal selection prior to the memory period in ECES trials, since neural spiking in PRR and PMd were predominantly selective for the pending spatial motor goal, not the preceding spatial cue, during the memory period. This can be seen from the example neurons in Fig. S2 and corresponding analyses in (Westendorff et al. 2010), consistently with earlier studies (Crammond and Kalaska 1994; Gail and Andersen 2006; Gail et al. 2009). While neural selectivity based on spiking does not necessarily always match selectivity based on LFP in PRR (Kuang et al. 2016), the observed selectivity of the spiking here is informative about the information contained in the neural activities of both, PRR and PMd. Therefore, the lack of functional interaction despite neural evidence for cue integration

and motor-goal selection at the time of the pre-cue contradicts the motor-goal selection hypothesis.

Based on timing, one could argue that frontal-to-parietal interaction only occurs during definite (go-cue), but not preliminary (pre-cue) motor-goal selection. Indeed, functional interaction from PMd to PRR was high around the time of commitment to a definite motor goal. Yet, the strength of this phasic interaction depended on the knowledge that the monkeys had during the preceding memory period. This suggests that the observed interaction might be partially but not sufficiently explained by an unspecific frontal-to-parietal interaction associated with processes like final motor-goal selection, release of response inhibition, reach initiation, or efference copy (Kalaska and Crammond 1995; Battaglia-Mayer et al. 2014). An extension of the present task which includes a second delay period would allow dissociating definite motor-goal selection from these alternative possibilities.

### Frontal-to-Parietal Interaction in Low-frequency LFP During Spatial WM Retrieval

Around the time of commitment to the movement with the go-cue, low-frequency frontal-to-parietal interaction scaled with the preceding spatial WM load. Interaction was strongest when monkeys needed to retrieve trial-specific spatial information about the currently valid motor-goal from WM. A difference in cognitive demand is also indicated by longer RTs of both monkeys in these 2 conditions of WM retrieval (except for antireaches in monkey A, which are slow and equal in all cueing conditions). These systematic RT modulations correlated with the level of DI confirming that modulation of frontal-to-parietal interaction in low-frequency LFP in our experiment corresponded to differences in spatial WM retrieval.

The idea of "top-down" signaling for WM retrieval is not new, and in monkeys is being studied in great detail particularly for object association memory in the temporal lobe (see (Miyashita 2004; Hirabayashi and Miyashita 2014) for review). For example, voluntary recall of memory in a visual categorization task apparently depends on cortico-cortical projections from prefrontal cortex to the inferior temporal lobe. Callosal transection experiments in monkeys showed that only as long as the anterior corpus callosum was intact and allowed trans-hemispheric communication in the frontal lobe, monkeys performed well and inferiotemporal neurons still encoded information about memorized ipsilateral visual cues (Tomita et al. 1999). Also, during short-term visual memory maintenance, LFP signals between visual area V4 and lateral prefrontal cortex synchronize at low signal frequencies (Liebe et al. 2012). While details about activation of object memories in the micro-circuitry of the temporal lobe are increasingly well understood (Hirabayashi et al. 2013), the role of top-down projections for memory retrieval is not clear yet (Hirabayashi and Miyashita 2014).

Spatial as opposed to object WM processing, instead, is supported in a separate network linking lateral prefrontal cortex with the widespread frontoparietal sensorimotor system according to monkey (Wilson et al. 1993; Goldman-Rakic 1995) and human physiology (Belger et al. 1998; Wager and Smith 2003; Sack et al. 2008; Sreenivasan et al. 2014). Accordingly, sustained spatial selective neural responses during memory-guided planning of movements are found throughout posterior parietal, premotor, and lateral prefrontal cortex, supporting the notion that sustained activities in the FPN are a form of prospective memory used for (spatial) planning behavior. And existing empirical data point to a strong need for functional frontoparietal interaction during spatial WM processing in primates (Wager and Smith 2003; Sauseng et al. 2005, 2010; Sreenivasan et al. 2014). Yet, the mutual responsibilities and functional interactions in this large-scale spatial WM network are not understood and mechanistic explanations of processes like encoding, active maintenance, or retrieval do not exist.

Especially evidence at the local neuronal level so far is scarce, but will be important to identify differences between subregions in the frontal and the parietal lobes. Recently, Crowe and colleagues (Crowe et al. 2013) showed prefrontal-to-parietal functional interaction in a category selection task which included WM. The interaction occurred while and after the monkeys had to integrate a spatial cue with a spatial category cue. The observed interaction could be the signature of the category selection process itself, or of the encoding of the resulting category information into WM to bridge the pending memory period. Computational models and human imaging data, on the other hand, suggest that prefrontal projections could help boosting WM capacity in the memory-storing parietal cortex (Edin et al. 2009). Rather than prefrontal cortex, our study focused on premotor cortex which shares high similarity in single neuron selectivity during rule-guided reach planning (Gail et al. 2009; Chakrabarti et al. 2014). Our data suggest that premotor-to-parietal interaction particularly at low signal frequencies is indicative of motor-goal retrieval from spatial WM during memory-guided reaching in monkeys, while reverberating beta-frequency activity in parietal cortex could support storage, with limitations, as discussed below.

Our interpretation does not contradict previous reports of directed premotor-to-parietal interaction in monkey at low signal frequencies, but add a new perspective to it. Similar to our data, Pesaran and colleagues showed transient low-frequency functional interaction from PMd to PRR at the time of final motor goal selection. Interaction was stronger during free search of a reach goal among multiple visual target stimuli identical in shape compared with instructed reach goal selection among target stimuli different in shape (Pesaran et al. 2008). While the observed interaction can be and was interpreted as signature of a decision making process, it is interesting to note that the 2 task conditions also differ in terms of required WM retrieval. The free-search condition was a foraging task in which monkeys needed to recall the previously visited target positions, hence a spatial WM task. In the instructed condition, instead, animals needed to recall the learned sequence of stimulus shapes, more similar to an object or sequence memory task. Therefore, the observed enhanced premotor-to-parietal interaction could have resulted from selective engagement of the spatial WM system in the free-search task. In the same 2 brain areas, partial spike-field coherence was shown to be strong at low signal frequencies around the time of reach execution (Stetson and Andersen 2014). An interpretation of this signal was not provided, but since it occurred after the end of spatial WM period, it could have been indicative of spatial WM retrieval as well.

To our surprise, we did not observe context dependency of the premotor-to-parietal functional interaction. We had expected such dependency since at the level of single neuron spiking both areas in the same experiment had shown differences in the latency of neural motor-goal selectivity between pro and antireaches (Westendorff et al. 2010). And previous observations of latency differences between parietal (LIP) and prefrontal Broadmann areas 47 and 8a (involved in WM) in a proanti memory saccade tasks suggested the possibility of a prefrontal-to-parietal context-contingent signal responsible of switching the sensorimotor transformations in parietal cortex (Barash 2003).

### Strength of Parietal-to-Frontal Interaction in Beta-Range LFP Not Specific for Content During WM Maintenance

The 4 cueing conditions of our task required the monkeys to maintain different WM contents, and we asked if DI would support WM maintenance in a content-specific way. While sustained DI from parietal to frontal cortex during the memory period was strongly dominating, it was not content-specific since it did not differ between cueing conditions. Coherent LFP signals were previously associated with WM maintenance during spatial saccade planning within the posterior parietal cortex (Pesaran et al. 2002), during object memory in the ventral visual stream (Tallon-Baudry et al. 2004) and larger-scale frontoparietal cortex (Brovelli et al. 2004; Salazar et al. 2012). Further, LFP-beta within PRR is known to be modulated by task-relevant spatial parameters during reach tasks with instructed delay, and therefore could support content-specific WM maintenance during reach planning (Scherberger et al. 2005; Kuang et al. 2016). LFP-beta in PMd, instead, while known to be spatially selective during evoked potentials (Mehring et al. 2003; O'Leary and Hatsopoulos 2006), was strongly attenuated in power during sustained memory phases, especially compared with PRR (Fig. 2 and (Chakrabarti et al. 2014)). Correspondingly, Salazar and colleagues showed that beta-range interaction was dominated by parietal-to-frontal influences (parietal senders, frontal receivers), and that frontoparietal beta-frequency coherence was content-specific (Salazar et al. 2012). Yet, since coherence is not a directed measure, it remained unclear from this previous study if content-specificity was also given for the DI from parietal to frontal cortex.

In our data, DI at beta frequencies, in stark contrast to our observed low-frequency interaction, was independent of WM content. The strength of DI-beta did not vary with the cueing condition. Instead, DI-beta was characteristic for movement-withholding states, that is, instructed delays, even without any trial-specific information being specified yet (fixation period of all cueing conditions). This means, while reverberating oscillatory activities at beta frequencies, that is, local beta-range signal power, in principle might well be suited to actively maintain spatial WM content in posterior parietal cortex (Jensen et al. 2002; Van Der Werf et al. 2008; Palva et al. 2010; Chakrabarti et al. 2014), the strength of DI with premotor cortex at beta-range frequencies during WM maintenance is lacking such content-specificity. This could have 2 reasons. First, Stetson and Andersen (Stetson and Andersen 2014) described beta rhythms to be antiphasic between PRR and PMd, and argued against the idea that beta-range signals support communication across areas. This interpretation could connect with the fact that it might not be necessary to consider reverberating oscillatory beta activities between brain areas to explain WM maintenance in the FPN, since local network mechanisms within a single cortical area could allow re-activation of weak short-term memory representations (here: in premotor) for postponed decisions (Lemus et al. 2007; Martinez-Garcia et al. 2011). The non-specific input to trigger such re-activation process postulated in these previous studies might be linked to the frontoparietal low-frequency interaction observed here, but this is speculative. Second, one does not have to go as far as to reject the idea of sustained communication completely, only because the measure of interaction used is not modulated by content. If DI based on LFP-beta indicated whether a parieto-frontal communication channel is active or inactive, while at the same time being blind to the content of the communication, then this would explain the lack of modulation in strength of parieto-frontal interaction between cueing conditions. What is counter-intuitive about this view, however, is that parieto-frontal communication seems to be interrupted when new stimuli are presented or when the animal moves, that is, at times when dorsal stream processing seems particularly relevant. Ultimately, information content of sustained parieto-frontal DI and its function remain unclear.

### Bidirectional Communication in Separate Frequency Bands

Our results suggest that different frequency bands support distinct channels for directed communication, with beta/gamma-band activities dominating parietal-to-frontal influences, and low-frequency activities dominating frontal-to-parietal influences. In contrast, in visual cortical areas beta-band or lower gamma-range activities dominate top-down influences, (higher) gamma and theta band frequencies bottom-up processing (Buschman and Miller 2007; Bastos et al. 2015; Bressler and Richter 2015). Apparently, while an equivalent principle of separate communication channels seems to be implemented in visual and sensorimotor cortical networks, different roles seem to be assigned to different signal frequencies in both systems. Notably, the equivalent task of planning memory-guided center-out saccades and reaches, respectively, reveal distinct dominant signal frequencies in otherwise corresponding sensorimotor areas, namely gamma-range signals during saccade planning in area LIP (Pesaran et al. 2002) and beta-range signals during reach planning area MIP (PRR) (Scherberger et al. 2005). Future studies will have to show in how far differences in predominant signal frequency might be attributable to distinct processing in the frontoparietal skeletomotor system versus the oculomotor system, or to other factors. In the context of WM processing, a recent human anatomical study might allow us to indirectly link the dominant frequencies to different communication pathways. Direct (corticocortical) frontoparietal pathway strengths across individuals correlated better with WM maintenance capacity, while indirect (subcortical) pathway strength correlated with WM update capacity (Ekman et al. 2016). This would argue that at least the observed beta-range interaction during WM maintenance is mediated by corticocortical processing.

### Conclusion

We identified DI between premotor area PMd and posterior parietal area PRR at 2 distinct signal frequencies, likely serving cognitive control during memory-guided rule-dependent reaching. Frontal-to-parietal interaction at low signal frequencies correlated with the time of initiation of a reach response and was particularly strong during spatial WM retrieval, here retrieval of motor goal location. Additional parietal-to-frontal interaction at beta frequencies could support retention of WM ("hold"), albeit in a content-independent manner.

## Authors' Contributions

P.M.-V. wrote the analysis programs and performed the analyses. A.G. designed the experiments and wrote the manuscript together with P.M.-V.

## Supplementary Material

Supplementary material is available at *Cerebral Cortex* online.

## Funding

This work was supported by the Federal Ministry for Education and Research (BMBF, Germany) grants 01GQ0814 (Bernstein Focus for Neurotechnology) and 01GQ1005C (Bernstein Center for Computational Neuroscience), and the German Research Foundation (DFG, Germany) grant SFB-889 (Cellular Mechanisms of Sensory Processing) awarded to A.G.

## Notes

The authors thank Christian Klaes and Steffi Westendorff for the data acquisition and sharing this database from previous publications of corresponding spike data, Shubo Chakrabarti for his support with the database, and Suresh Krishna for discussion and feedback on earlier versions of the manuscript. *Conflict of Interest*: None declared.

## References

Akaike H. 1968. On the use of a linear model for the identification of feedback systems. Ann Inst Stat Math. 20:425–439.

Andersen RA, Cui H. 2009. Intention, action planning, and decision making in parietal-frontal circuits. Neuron. 63:568–583.

Bakola S, Gamberini M, Passarelli L, Fattori P, Galletti C. 2010. Cortical connections of parietal field PEc in the macaque: linking vision and somatic sensation for the control of limb action. Cereb Cortex. 20:2592–2604.

Barash S. 2003. Paradoxical activities: insight into the relationship of parietal and prefrontal cortices. Trends Neurosci. 26: 582–589.

Bastos AM, Vezoli J, Bosman CA, Schoffelen JM, Oostenveld R, Dowdall JR, De Weerd P, Kennedy H, Fries P. 2015. Visual areas exert feedforward and feedback influences through distinct frequency channels. Neuron. 85:390–401.

Battaglia-Mayer A, Buiatti T, Caminiti R, Ferraina S, Lacquaniti F, Shallice T. 2014. Correction and suppression of reaching movements in the cerebral cortex: physiological and neuropsychological aspects. Neurosci Biobehav Rev. 42:232–251.

Belger A, Puce A, Krystal JH, Gore JC, Goldman-Rakic P, McCarthy G. 1998. Dissociation of mnemonic and perceptual processes during spatial and nonspatial working memory using fMRI. Hum Brain Mapp. 6:14–32.

Bressler SL, Richter CG. 2015. Interareal oscillatory synchronization in top-down neocortical processing. Curr Opin Neurobiol. 31:62–66.

Brovelli A, Ding M, Ledberg A, Chen Y, Nakamura R, Bressler SL. 2004. Beta oscillations in a large-scale sensorimotor cortical network: directional influences revealed by Granger causality. Proc Natl Acad Sci USA. 101:9849–9854.

Buschman TJ, Miller EK. 2007. Top-down versus bottom-up control of attention in the prefrontal and posterior parietal cortices. Science. 315:1860–1862.

Caminiti R, Genovesio A, Marconi B, Mayer AB, Onorati P, Ferraina S, Mitsuda T, Giannetti S, Squatrito S, Maioli MG, et al. 1999. Early coding of reaching: frontal and parietal association connections of parieto-occipital cortex. Eur J Neurosci. 11:3339–3345.

Chafee MV, Goldman-Rakic PS. 2000. Inactivation of parietal and prefrontal cortex reveals interdependence of neural activity during memory-guided saccades. J Neurophysiol. 83: 1550–1566.

Chakrabarti S, Martinez-Vazquez P, Gail A. 2014. Synchronization patterns suggest different functional organization in parietal reach region and dorsal premotor cortex. J Neurophysiol. 112: 3138–3153.

Chicharro D. 2011. On the spectral formulation of Granger causality. Biol Cybern. 105:331–347.

Cisek P. 2012. Making decisions through a distributed consensus. Curr Opin Neurobiol. 22:927–936.

Cisek P, Kalaska JF. 2005. Neural correlates of reaching decisions in dorsal premotor cortex: specification of multiple direction choices and final selection of action. Neuron. 45:801–814.

Cisek P, Kalaska JF. 2010. Neural mechanisms for interacting with a world full of action choices. Annu Rev Neurosci. 33:269–298.

Coallier E, Michelet T, Kalaska JF. 2015. Dorsal premotor cortex: neural correlates of reach target decisions based on a color-location matching rule and conflicting sensory evidence. J Neurophysiol. 113:3543–3573.

Colby CL, Gattass R, Olson CR, Gross CG. 1988. Topographical organization of cortical afferents to extrastriate visual area PO in the macaque: a dual tracer study. J Comp Neurol. 269: 392–413.

Crammond DJ, Kalaska JF. 1994. Modulation of preparatory neuronal activity in dorsal premotor cortex due to stimulus-response compatibility. J Neurophysiol. 71:1281–1284.

Crowe DA, Goodwin SJ, Blackman RK, Sakellaridi S, Sponheim SR, Macdonald AW, Chafee MV. 2013. Prefrontal neurons transmit signals to parietal neurons that reflect executive control of cognition. Nat Neurosci. 16:1484–1491.

Dotson NM, Salazar RF, Gray CM. 2014. Frontoparietal correlation dynamics reveal interplay between integration and segregation during visual working memory. J Neurosci. 34: 13600–13613.

Edin F, Klingberg T, Johansson P, McNab F, Tegner J, Compte A. 2009. Mechanism for top-down control of working memory capacity. Proc Natl Acad Sci USA. 106:6802–6807.

Ekman M, Fiebach CJ, Melzer C, Tittgemeyer M, and Derrfuss J. 2016. Different roles of direct and indirect frontoparietal pathways for individual working memory capacity. J Neurosci. 36:2894–2903.

Funahashi S, Bruce CJ, Goldman-Rakic PS. 1989. Mnemonic coding of visual space in the monkey's dorsolateral prefrontal cortex. J Neurophysiol. 61:331–349.

Fuster JM. 2001. The prefrontal cortex—an update: time is of the essence. Neuron. 30:319–333.

Fuster JM. 2009. Cortex and memory: emergence of a new paradigm. J Cogn Neurosci. 21:2047–2072.

Gail A, Andersen RA. 2006. Neural dynamics in monkey parietal reach region reflect context-specific sensorimotor transformations. J Neurosci. 26:9376–9384.

Gail A, Klaes C, Westendorff S. 2009. Implementation of spatial transformation rules for goal-directed reaching via gain modulation in monkey parietal and premotor cortex. J Neurosci. 29:9490–9499.

Gamberini M, Passarelli L, Fattori P, Zucchelli M, Bakola S, Luppino G, Galletti C. 2009. Cortical connections of the visuomotor parietooccipital area V6Ad of the macaque monkey. J Comp Neurol. 513:622–642.

Geweke J. 1982. Measurement of linear dependence and feedback between multiple time series. J Am Stat Assoc. 77: 304–313.

Ghosh S, Gattera R. 1995. A comparison of the ipsilateral cortical projections to the dorsal and ventral subdivisions of the macaque premotor cortex. Somatosens Mot Res. 12: 359–378.

Goldman-Rakic PS. 1995. Cellular basis of working memory. Neuron. 14:477–485.

Graf W, Prevosto V, Ugolini G 2006. Differences in disynaptic fronto-parietal input from arcuate and premotor cortex to medial (MIP/VIPm) and lateral (VIPl/LIPv) intraparietal areas, revealed by retrograde transneuronal transfer of rabies virus. Society for Neuroscience.Atlanta (GA). Program No. 242.17. Online.

Hirabayashi T, Miyashita Y. 2014. Computational principles of microcircuits for visual object processing in the macaque temporal cortex. Trends Neurosci. 37:178–187.

Hirabayashi T, Takeuchi D, Tamura K, Miyashita Y. 2013. Functional microcircuit recruited during retrieval of object association memory in monkey perirhinal cortex. Neuron. 77:192–203.

Jensen O, Gelfand J, Kounios J, Lisman JE. 2002. Oscillations in the alpha band (9-12 Hz) increase with memory load during retention in a short-term memory task. Cereb Cortex. 12: 877–882.

Johnson PB, Ferraina S, Bianchi L, Caminiti R. 1996. Cortical networks for visual reaching: physiological and anatomical organization of frontal and parietal lobe arm regions. Cereb Cortex. 6:102–119.

Kalaska JF, Crammond DJ. 1995. Deciding not to GO: neuronal correlates of response selection in a GO/NOGO task in primate premotor and parietal cortex. Cereb Cortex. 5:410–428.

Kalaska JF, Scott SH, Cisek P, Sergio LE. 1997. Cortical control of reaching movements. Curr Opin Neurobiol. 7:849–859.

Kaminski MJ, Blinowska KJ. 1991. A new method of the description of the information flow in the brain structures. Biol Cybern. 65:203–210.

Kaminski M, Ding M, Truccolo WA, Bressler SL. 2001. Evaluating causal relations in neural systems: granger causality, directed transfer function and statistical assessment of significance. Biol Cybern. 85:145–157.

Klaes C, Schneegans S, Schoner G, Gail A. 2012. Sensorimotor learning biases choice behavior: a learning neural field model for decision making. PLoS Comput Biol. 8:e1002774.

Klaes C, Westendorff S, Chakrabarti S, Gail A. 2011. Choosing goals, not rules: deciding among rule-based action plans. Neuron. 70:536–548.

Kuang S, Morel P, Gail A. 2016. Planning movements in visual and physical space in monkey posterior parietal cortex. Cereb Cortex. 26:731–747.

Lemus L, Hernandez A, Luna R, Zainos A, Nacher V, Romo R. 2007. Neural correlates of a postponed decision report. Proc Natl Acad Sci USA. 104:17174–17179.

Lewis JW, Van Essen DC. 2000a. Corticocortical connections of visual, sensorimotor, and multimodal processing areas in the parietal lobe of the macaque monkey. J Comp Neurol. 428:112–137.

Lewis JW, Van Essen DC. 2000b. Mapping of architectonic subdivisions in the macaque monkey, with emphasis on parieto-occipital cortex. J Comp Neurol. 428:79–111.

Liebe S, Hoerzer GM, Logothetis NK, Rainer G. 2012. Theta coupling between V4 and prefrontal cortex predicts visual short-term memory performance. Nat Neurosci. 15:456.

Luetkepohl H. 2005. New Introduction to Multiple Time Series Analysis. Berlin Heidelberg: Springer.

Luppino G, Calzavara R, Rozzi S, Matelli M. 2001. Projections from the superior temporal sulcus to the agranular frontal cortex in the macaque. Eur.J Neurosci. 14:1035–1040.

Luppino G, Rozzi S, Calzavara R, Matelli M. 2003. Prefrontal and agranular cingulate projections to the dorsal premotor areas F2 and F7 in the macaque monkey. Eur J Neurosci. 17:559–578.

Marconi B, Genovesio A, Battaglia-Mayer A, Ferraina S, Squatrito S, Molinari M, Lacquaniti F, Caminiti R. 2001. Eye-hand coordination during reaching. I. Anatomical relationships between parietal and frontal cortex. Cereb Cortex. 11:513–527.

Markov NT, Ercsey-Ravasz MM, Ribeiro Gomes AR, Lamy C, Magrou L, Vezoli J, Misery P, Falchier A, Quilodran R, Gariel MA, et al. 2014. A weighted and directed interareal connectivity matrix for macaque cerebral cortex. Cereb Cortex. 24: 17–36.

Martinez-Garcia M, Rolls ET, Deco G, Romo R. 2011. Neural and computational mechanisms of postponed decisions. Proc Natl Acad Sci USA. 108:11626–11631.

Matelli M, Govoni P, Galletti C, Kutz DF, Luppino G. 1998. Superior area 6 afferents from the superior parietal lobule in the macaque monkey. J Comp Neurol. 402:327–352.

Matelli M, Luppino G, Rizzolatti G. 1991. Architecture of superior and mesial area 6 and the adjacent cingulate cortex in the macaque monkey. J Comp Neurol. 311:445–462.

Mehring C, Rickert J, Vaadia E, Cardosa de OS, Aertsen A, Rotter S. 2003. Inference of hand movements from local field potentials in monkey motor cortex. Nat Neurosci. 6: 1253–1254.

Miller EK, Cohen JD. 2001. An integrative theory of prefrontal cortex function. Annu Rev Neurosci. 24:167–202.

Miyashita Y. 2004. Cognitive memory: cellular and network machineries and their top-down control. Science. 306: 435–440.

Moisa M, Siebner HR, Pohmann R, Thielscher A. 2012. Uncovering a context-specific connectional fingerprint of human dorsal premotor cortex. J Neurosci. 32:7244–7252.

Mulliken GH, Musallam S, Andersen RA. 2008. Forward estimation of movement state in posterior parietal cortex. Proc Natl Acad Sci USA. 105:8170–8177.

Munoz DP, Everling S. 2004. Look away: the anti-saccade task and the voluntary control of eye movement. Nat Rev Neurosci. 5:218–228.

Nacher V, Ledberg A, Deco G, Romo R. 2013. Coherent delta-band oscillations between cortical areas correlate with decision making. Proc Natl Acad Sci USA. 110:15085–15090.

Neumaier A. 2001. Estimation of parameters and eigenmodes of multivariate auroregressive models. ACM Trans Math Softw. 27:27–57.

Osborne AR, Kirwan AD, Provenzale A, Bergamasco L. 1986. A search for chaotic behavior in large and mesoscale motions in the Pacific Ocean. Physica D. 23:75–83.

O'Leary JG, Hatsopoulos NG. 2006. Early visuomotor representations revealed from evoked local field potentials in motor and premotor cortical areas. J Neurophysiol. 96:1492–1506.

Palva JM, Monto S, Kulashekhar S, Palva S. 2010. Neuronal synchrony reveals working memory networks and predicts individual memory capacity. Proc Natl Acad Sci USA. 107: 7580–7585.

Passarelli L, Rosa MG, Gamberini M, Bakola S, Burman KJ, Fattori P, Galletti C. 2011. Cortical connections of area V6Av in the macaque: a visual-input node to the eye/hand coordination system. J Neurosci. 31:1790–1801.

Pesaran B, Nelson MJ, Andersen RA. 2008. Free choice activates a decision circuit between frontal and parietal cortex. Nature. 453:406–409.

Pesaran B, Pezaris JS, Sahani M, Mitra PP, Andersen RA. 2002. Temporal structure in neuronal activity during working memory in macaque parietal cortex. Nat Neurosci. 5: 805–811.

Petrides M. 1982. Motor conditional associative-learning after selective prefrontal lesions in the monkey. Behav Brain Res. 5:407–413.

Petrides M, Pandya DN. 1999. Dorsolateral prefrontal cortex: comparative cytoarchitectonic analysis in the human and the macaque brain and corticocortical connection patterns. Eur J Neurosci. 11:1011–1036.

Praamstra P, Kourtis D, Nazarpour K. 2009. Simultaneous preparation of multiple potential movements: opposing effects of spatial proximity mediated by premotor and parietal cortex. J Neurophysiol. 102:2084–2095.

Rawle CJ, Miall RC, Praamstra P. 2012. Frontoparietal theta activity supports behavioral decisions in movement-target selection. Front Hum Neurosci. 6:138.

Rowe JB, Passingham RE. 2001. Working memory for location and time: activity in prefrontal area 46 relates to selection rather than maintenance in memory. NeuroImage. 14: 77–86.

Sack AT, Jacobs C, De Martino F, Staeren N, Goebel R, Formisano E. 2008. Dynamic premotor-to-parietal interactions during spatial imagery. J Neurosci. 28:8417–8429.

Salazar RF, Dotson NM, Bressler SL, Gray CM. 2012. Content-specific fronto-parietal synchronization during visual working memory. Science. 338:1097–1100.

Sauseng P, Griesmayr B, Freunberger R, Klimesch W. 2010. Control mechanisms in working memory: a possible function of EEG theta oscillations. Neurosci Biobehav Rev. 34: 1015–1022.

Sauseng P, Klimesch W, Schabus M, Doppelmayr M. 2005. Fronto-parietal EEG coherence in theta and upper alpha reflect central executive functions of working memory. Int J Psychophysiol. 57:97–103.

Scherberger H, Jarvis MR, Andersen RA. 2005. Cortical local field potential encodes movement intentions in the posterior parietal cortex. Neuron. 46:347–354.

Schlag-Rey M, Amador N, Sanchez H, Schlag J. 1997. Antisaccade performance predicted by neuronal activity in the supplementary eye field. Nature. 390:398–401.

Shipp S, Blanton M, Zeki S. 1998. A visuo-somatomotor pathway through superior parietal cortex in the macaque monkey: cortical connections of areas V6 and V6A. Eur J Neurosci. 10:3171–3193.

Snyder LH, Batista AP, Andersen RA. 2000. Intention-related activity in the posterior parietal cortex: a review. Vision Res. 40:1433–1441.

Sreenivasan KK, Curtis CE, D'Esposito M. 2014. Revisiting the role of persistent neural activity during working memory. Trends Cogn Sci. 18:82–89.

Stetson C, Andersen RA. 2014. The parietal reach region selectively anti-synchronizes with dorsal premotor cortex during planning. J Neurosci. 34:11948–11958.

Stoet G, Snyder LH. 2004. Single neurons in posterior parietal cortex of monkeys encode cognitive set. Neuron. 42:1003–1012.

Takahashi DY, Baccala LA, Sameshima K. 2010. Information theoretic interpretation of frequency domain connectivity measures. Biol Cybern. 103:463–469.

Tallon-Baudry C, Mandon S, Freiwald WA, Kreiter AK. 2004. Oscillatory synchrony in the monkey temporal lobe correlates with performance in a visual short-term memory task. Cereb Cortex. 14:713–720.

Tanné-Gariépy J, Rouiller EM, Boussaoud D. 2002. Parietal inputs to dorsal versus ventral premotor areas in the macaque monkey: evidence for largely segregated visuomotor pathways. Exp Brain Res. 145:91–103.

Theiler J, Eubank S, Longtin A, Galdrikian B, Farmer JD. 1992. Testing for nonlinearity in time series: the method of surrogate data. Physica D. 58:77–94.

Tomita H, Ohbayashi M, Nakahara K, Hasegawa I, Miyashita Y. 1999. Top-down signal from prefrontal cortex in executive control of memory retrieval. Nature. 401:699–703.

Toni I, Rushworth MF, Passingham RE. 2001. Neural correlates of visuomotor associations. Spatial rules compared with arbitrary rules. Exp Brain Res. 141:359–369.

Van Der Werf J, Jensen O, Fries P, Medendorp WP. 2008. Gamma-band activity in human posterior parietal cortex encodes the motor goal during delayed prosaccades and antisaccades. J Neurosci. 28:8397–8405.

Wager TD, Smith EE. 2003. Neuroimaging studies of working memory: a meta-analysis. Cogn Affect Behav Neurosci. 3: 255–274.

Wallis JD, Anderson KC, Miller EK. 2001. Single neurons in prefrontal cortex encode abstract rules. Nature. 411:953–956.

Wallis JD, Miller EK. 2003. From rule to response: neuronal processes in the premotor and prefrontal cortex. J Neurophysiol. 90:1790–1806.

Westendorff S, Klaes C, Gail A. 2010. The cortical timeline for deciding on reach motor goals. J Neurosci. 30:5426–5436.

Wilson FA, Scalaidhe SP, Goldman-Rakic PS. 1993. Dissociation of object and spatial processing domains in primate prefrontal cortex. Science. 260:1955–1958.

Wise SP, Boussaoud D, Johnson PB, Caminiti R. 1997. Premotor and parietal cortex: corticocortical connectivity and combinatorial computations. Annu Rev Neurosci. 20:25–42.

Zhang M, Barash S. 2004. Persistent LIP activity in memory antisaccades: working memory for a sensorimotor transformation. J Neurophysiol. 91:1424–1441.